Available online at www.sciencedirect.com
SCIENCE DIRECT
Journal of Molecular Catalysis A: Chemical 247 (2006) 189–198
JOURNAL OF MOLECULAR CATALYSIS A: CHEMICAL
www.elsevier.com/locate/molcata

Formation and adsorption properties of the bridging sulfur vacancies at the ($\bar{1}$ 0 1 0) edge of $Mo_{27}S_{(54-x)}$: A theoretical study

Guisheng Wu [a,*], Kangnian Fan [a], B. Delmon [b], Yong-Wang Li [c]

[a] *Department of Chemistry, Fudan University, Shanghai, PR China*
[b] *Unité de Catalyse et Chimie des Matériaux Divisés, Université Catholique de Louvain, B-1348 Louvain-la-Neuve, Belgium*
[c] *The State Key Laboratory of Coal Conversion, Institute of Coal Chemistry, Chinese Academy of Science, Taiyuan 030001, China*

Received 1 September 2005; received in revised form 24 November 2005; accepted 24 November 2005
Available online 6 January 2006

Abstract

The structure and adsorption of $Mo_{27}S_{(54-x)}$ (x = 1–6) clusters have been investigated using density functional theory method. It was found that considerable relaxation occurred at the ($\bar{1}$ 0 1 0) edge. The activity has been analyzed on the basis of frontier molecular orbital properties. The results suggest that the possible catalytic sites might be situated between two vicinal 4-fold coordinative unsaturated site CUS. The formation of $Mo_{27}S_{(54-x)}$ (x = 4–6) from $Mo_{27}S_{54}$ is easy in the presence of atomic hydrogen, but difficult under molecular hydrogen. But the situation is different from the case of $Mo_{27}S_{(54-x)}$ formation (x = 1–3) that is facile under both the atomic and molecular hydrogen reagent (under the normal HYD/HDS condition). The adsorption of thiophene at various vacancies on the ($\bar{1}$ 0 1 0) edge of MoS_2 represents that thiophene is unstable to flatly adsorb at the vacancy of $Mo_{27}S_{50}$. Although uprightly adsorbed thiophene is adsorbed weakly, the flatly adsorbed thiohene is strongly activated when adsorbed between two vicinal 4-fold CUS (**9**, **10**). On the basis of Hirshfeld charge analysis, the donation and back-donation between the thiophene and the substrate might account for the activation of thiophene.

Keywords: ($\bar{1}$ 0 1 0) Edge of $Mo_{27}S_{(54-x)}$; The vacancies of $Mo_{27}S_{(54-x)}$; Thiophene adsorption; The vacancies of ($\bar{1}$ 0 1 0) of MoS_2; Donation and back-donation

1. Introduction

With the advent of increasingly stringent regulations of sulfur containing in oil products to less than 50 ppm, hydrodesulfurization (HDS) continues to be the focus of catalytic study. Molybdenum sulfide is believed to be the essential active element, which is promoted by other transition metals, such as cobalt and nickel. As one type of the sulfur containing impurities, thiophene is most averse to HDS and is often regarded as the target for the model study.

During the last three decades, a large number of experiments [1–4] have been carried out to clarify the active sites of molybdenum sulfide. It has proved that MoS_2 phase is highly dispersed with size of one to several nanometers in the supported catalysts [3]. In these dispersed particles, the boundaries in all directions are believed to provide the high intrinsic activity for HDS reaction. Furthermore, it has been shown experimentally that the removal of S atoms from a MoS_2 slab starts from the edge on which the formed CUS has strong adsorption affinity for thiophene and H_2S and is responsible for the thiophene HDS [5,6]. Although it is easy to form 2-fold CUS on the ($\bar{1}$ 0 1 0) edge of MoS_2 even under the atmosphere of H_2, the 2-fold CUSs may not activate the thiophene to the degree of cleaving S–C bond of thiophene [7,8]. More specifically, 3- and 4-fold CUSs formed at the edge of ($\bar{1}$ 0 1 0) together with SH groups seem to be responsible for the activation of HDS [7,9].

Apart from the extensive experimental studies, modern theoretical methods, especially density functional approaches, have also been employed to illuminate the nature of active sites of MoS_2 model catalyst as well as the adsorption of thiophene derivatives and hydrogen species on these sites. With the periodic models, Raybaud et al. [10–12] have carried out detailed studies on the surface structure of MoS_2 with and without promoter. Furthermore, the sulfur coverage of these surfaces in the gaseous H_2S/H_2 surroundings of working catalysts is also

* Corresponding author.
E-mail address: gswu@fudan.edu.cn (G. Wu).

1381-1169/$ – see front matter © 2005 Elsevier B.V. All rights reserved.
doi:10.1016/j.molcata.2005.11.050

determined according to the thermodynamical approach [13,14]. Nϕrskov and co-workers [15] have also calculated the structure and vacancies of MoS_2 as well as the H_2 adsorption on these sites using the periodic models, and indicated the S atoms located on the $(\bar{1}\,0\,1\,0)$ surface of MoS_2 are more active to H adsorption. In addition, the vacancy formation mechanisms on the $(\bar{1}\,0\,1\,0)$ surface of MoS_2 are validated on the basis of a periodic DFT study [16]. Even so, the periodically repeated arrangement of chosen units seems not to reflect the geometries of MoS_2 slabs in the real catalysts which are actually finite in size and have boundaries in all directions. In addition, the roles of atomic hydrogen and proton are not also taken into account. Using cluster model, Li et al. [8] optimize the structure of $Mo_{27}S_{54}$ cluster whose size is similar to that in supported catalysts. They pointed out the Mo sites situated in $(\bar{1}\,0\,1\,0)$ edge are more active for HDS reaction when the sulfur atoms blocking the Mo atoms are removed. Subsequently, Orita et al. [17] calculated the same cluster model with DFT method. The calculated structure data at the edge are in agreement with the data of real MoS_2 catalysts obtained using the EXAFS methods, further illustrating the rationality of the cluster model of $Mo_{27}S_{54}$. Furthermore, the reduction of MoS_2 is also calculated using the cluster model. It is found that the terminal S atoms at the $(1\,0\,\bar{1}\,0)$ edge can be removed and the 2-fold CUS can form even by molecular hydrogen. With the presence of atomic hydrogen and increasing reaction temperature, the bridge sulfur sitting in the $(\bar{1}\,0\,1\,0)$ edge can be removed. Under much high temperature and atomic or protonic hydrogen, the S atoms on the basal plane can be removed, which can cause the structure of MoS_2 destroyed and should be avoided [7]. In addition, the adsorptions of thiophene and dibenzothiophene derivatives over MoS_2 nanoclusters have been widely investigated using density functional methods [18–21]. The active sites of these models are supposed as 2-fold coordinatively unsaturated sites (CUS) on the $(1\,0\,\bar{1}\,0)$ edge. However, little work dealing with thiophene adsorption at the CUS of the $(\bar{1}\,0\,1\,0)$ edge of MoS_2 has been published.

In order to model the catalytic activity of heterogeneous catalysts reasonably, two factors must be taken into account: (i) cluster size and (ii) changes of surface structure and composition. In this paper, both factors are considered, namely (i) a $Mo_{27}S_{54}$ model whose size is close to that of realistic catalysts and (ii) possible reduction process of the $(\bar{1}\,0\,1\,0)$ edge in the molecular and atomic hydrogen. Experimentally, it is found that the highly dispersed active MoS_2 supported clusters in practical catalysts have a size within 10–30 Å and build a mono-layered MoS_2 structure in some cases [22]. And we investigated the case of a fully structured $Mo_{27}S_{54}$ single slab with a size of 20 Å [19], which is close to that (10–30 Å) of the most highly dispersed MoS_2 in supported catalysts. At the same time, the possible removal processes of sulfur from the $(\bar{1}\,0\,1\,0)$ cluster edge and the structure of bridging sulfur vacancies are also calculated. Moreover, the adsorptions of thiophene at the different CUSs on $(\bar{1}\,0\,1\,0)$ edge of MoS_2 slab are also optimized. Both flat and the upright adsorption at the different sites are taken into account and the properties of the charge and electrons are also analyzed in details.

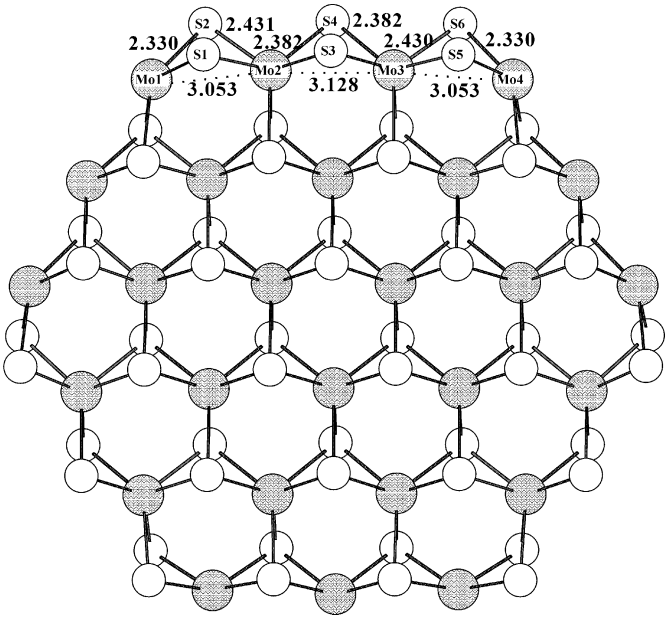

Fig. 1. Optimized structure of the $Mo_{27}S_{54}$ cluster.

2. Computational methods

Geometry optimizations are carried out with the DMol^3 program package [23–25] available in Materials Studio 2.2 of the Accelrys Inc. The doubled numerical basis set with a set of polarization functions is employed, which is comparable to the Gaussian 6-31G*. The effective core potential is used for Mo. The generalized gradient corrected (GGA) functional proposed by Perdew and Wang (PW91) is used, with the real space cutoff of atomic orbitals set at 5.5 Å and a smearing of 0.0005 to count the orbital occupancy. In geometry optimization, the BFGS routine, in which the gradients are computed numerically, is employed. For the numerical integration, the MEDIUM quality mesh size of the program is chosen. The tolerances of energy, gradient and displacement convergence are 2×10^{-5}, 1×10^{-2} and 1×10^{-2}, respectively. Because lower symmetry can be formed due to the relaxation of all atoms in the finite cluster, no symmetry conditions are employed here.

The initial coordinates of $Mo_{27}S_{54}$ (**1**) taken from the handbook of crystal structures [26] are used for geometry optimization. As shown in Fig. 1, **1** has a sandwiched structure with Mo atoms in the middle layer, doubly covered with two S planes. There are two individual bridging sulfurs with two Mo–S connections along the edge in **1**, and we have considered nine possibilities for bridging sulfur vacancies by successive sulfur removal. These cluster models can be designed as $Mo_{27}S_{(54-x)}$ (S_n), in which x is the total number of removed bridging sulfur and the subscript "n" is the sulfur position S_n of the bridging vacancy as indicated in the figure, respectively.

The CUS models employed here are obtained by removing the bridge sulfur at the $(\bar{1}\,0\,1\,0)$ edge of the $Mo_{27}S_{54}$ cluster. The optimized $Mo_{27}S_{54-x}$ structure is bonded with free thiophene and then is used as the initial structure of thiophene-$Mo_{27}S_{54-x}$. During the optimization of thiophene adsorbed on $Mo_{27}S_{54-x}$, the surface Mo and sulfur atoms of $Mo_{27}S_{54-x}$ and the atoms

composed of thiophene are allowed relaxed, while the rest atoms of the slab are held at the initial position. The adsorption energy of thiophene on $Mo_{27}S_{54}$ is given by Eq. (1):

$$\Delta E\,(\text{kcal/mol}) = E_{\text{thiophene-}Mo_{27}S_{54-x}} - E_{\text{thiophene}} - E_{Mo_{27}S_{54-x}} \quad (1)$$

where $E_{\text{thiophene-}Mo_{27}S_{54-x}}$, $E_{\text{thiophene}}$ and $E_{Mo_{27}S_{54-x}}$ are the total energy of the thiophene adsorbed on $Mo_{27}S_{54-x}$, optimized free thiophene and $Mo_{27}S_{54-x}$, respectively.

3. Results

3.1. $Mo_{27}S_{54-x}$

Fig. 2 represents the optimized structure of two distinct $Mo_{27}S_{53}$ clusters with sulfur vacancies at the corner (S_5, **2**) and edge site (S_3, **3**), respectively. The reference energies tabulated in Table 1 show that **2** is more stable than **3** by 10.7 kcal/mol. This indicates the stability of the corner 3-fold CUS. As compared to **1**, the Mo_3–Mo_4 distance in **2** becomes shorter (2.509 Å versus 3.053 Å), and the sulfur atom (S_6) moves to the Mo plane.

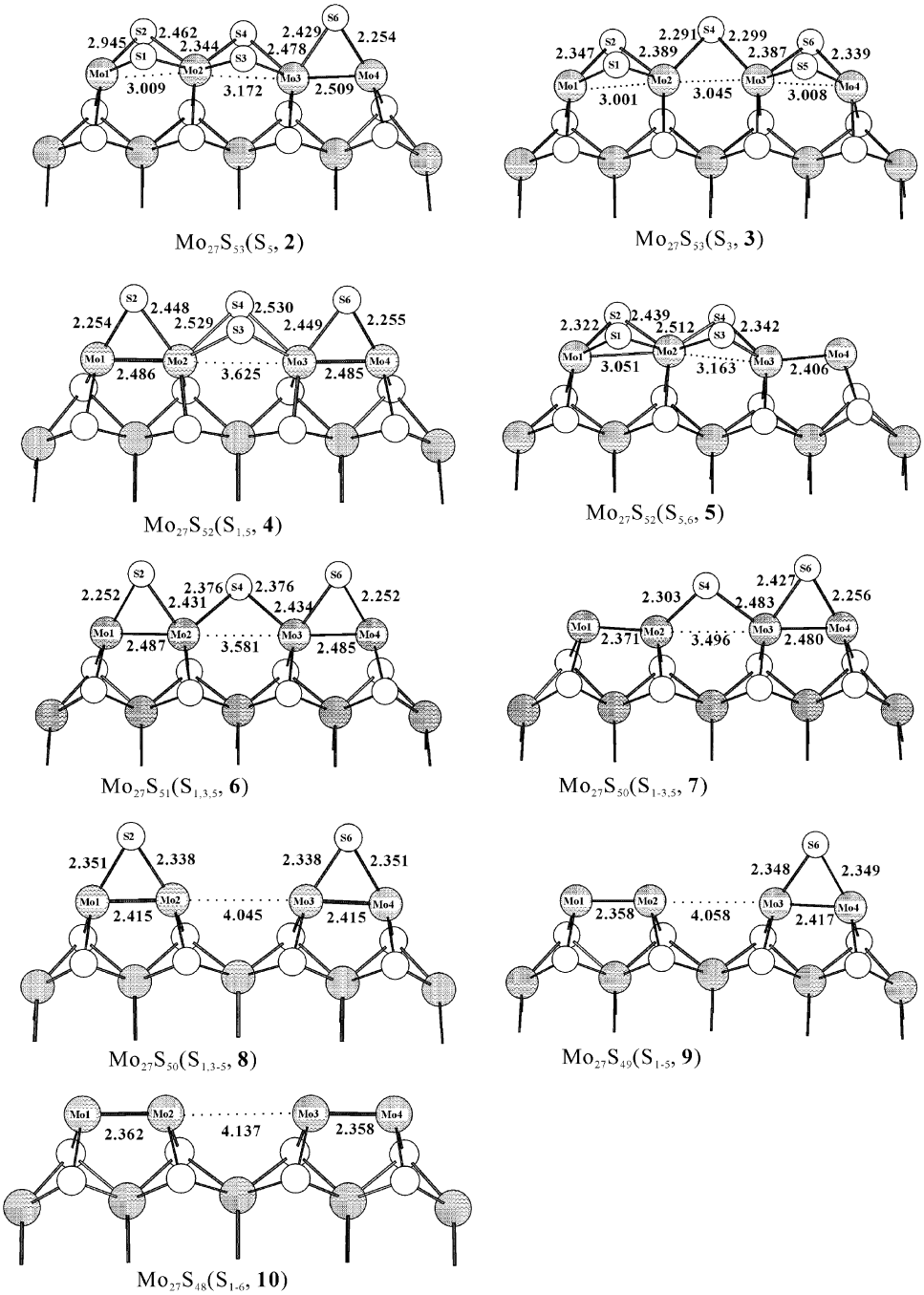

Fig. 2. The optimized structure of the $Mo_{27}S_{54-x}$ (x = 1–6).

Table 1
The reference energies (E_{ref}, au) to the total energy of $Mo_{27}S_{54}$ (−23354.43985 au) and the thiophene adsorption energy (E_{ad}, kcal/mol)

	E_{ref}	E_{ad}
$Mo_{27}S_{54}$ (**1**)	0	–
$Mo_{27}S_{53}$ (S_5, **2**)	398.2479	–
$Mo_{27}S_{53}$ (S_3, **3**)	398.2649	–
$Mo_{27}S_{52}$ ($S_{1,5}$, **4**)	796.4455	–
$Mo_{27}S_{52}$ ($S_{5,6}$, **5**)	796.5556	–
$Mo_{27}S_{51}$ ($S_{1,3,5}$, **6**)	1194.698	–
$Mo_{27}S_{50}$ ($S_{1–3,5}$, **7**)	1593.007	–
$Mo_{27}S_{50}$ ($S_{1,3–5}$, **8**)	1592.988	–
$Mo_{27}S_{49}$ ($S_{1–5}$, **9**)	1991.314	–
$Mo_{27}S_{48}$ ($S_{1–6}$, **10**)	2389.643	–
11	1040.562	−5.13
12	1040.596	16.77
13	1438.893	−10.18
14	1438.853	−35.20
15	1438.859	−30.92
16	1837.241	−7.78
17	1837.187	−41.45

In **3**, the Mo_2–Mo_3 distance also becomes shorter, but to a less extent than **2**.

Two $Mo_{27}S_{52}$ clusters obtained by removing two sulfur atoms from **1** at two different corners ($S_{1,5}$, **4**) and at the same corner ($S_{5,6}$, **5**) bridging the same Mo atoms, are shown in Fig. 2. In **4**, after the loss of two S atoms, $S_{2,6}$ is located in the same plane as the Mo atoms. Furthermore, the distance of Mo_1–Mo_2 (or Mo_3–Mo_4) is shortened to 2.485 Å, while that of Mo_2–Mo_3 is elongated to 3.625 Å. In **5**, both sulfur atoms ($S_{5,6}$) bridging Mo_3 and Mo_4 are removed, the distances of Mo_3–Mo_4 and Mo_2–Mo_3 are respectively shortened to 2.406, and elongated to 3.163 Å, compared to **1**. The reference energy in Table 1 shows that **4** is more stable than **5** by 69.1 kcal/mol. This indicates that the formation of 3-fold CUS is more energetically favored than the 4-fold CUS, respectively.

With removal of three sulfur atoms ($S_{1,3,5}$) from **1** results in structure **6**, as shown in Fig. 2. Similarly, the distance of Mo_1–Mo_2 (or Mo_3–Mo_4) is shortened to 2.485 Å, while that of Mo_2–Mo_3 is elongated to 3.581 Å. Furthermore, $S_{2,4,6}$ atoms move to the same plane as the Mo atoms.

As shown in Fig. 2, the removal of four bridging sulfur atoms at $S_{1–3,5}$ and $S_{1,3–5}$ from **1** results in **7** and **8**. Compared with **6**, **7** has slight changes, while the Mo_2–Mo_3 distance in **8** is further elongated to 4.045 Å. It is also noted that two 3-fold and one 4-fold CUSs are formed in **7**, while four 3-fold CUSs are formed in **8**. Furthermore, **8** is more stable than **7** by 11.4 kcal/mol, indicating the thermodynamic stability of 3-fold CUSs in general. Removal of $S_{1–5}$ and $S_{1–6}$ in **1** results in **9** and **10**, as shown in Fig. 2. Two 4-fold CUSs and two 3-fold CUSs are formed in **9**, and four 4-fold CUSs are formed in **10**. In **10**, the Mo_2–Mo_3 distance increases to 4.137 Å.

3.2. Thiophene adsorption at the vacancies of $Mo_{27}S_{54-x}$ (x = 4–6)

In addition to the formation of CUS, the adsorption of thiophene at the formed CUS has been also studied. The adsorptions of thiophene on the vacancies of $Mo_{27}S_{54-x}$ (x = 1–3) are calculated firstly, which display the very weak adsorption due to the strong (repulsion) between the thiophen and the S atoms of vacancies. Fig. 3 shows the optimized structures of thiophene adsorbed on the different vacancies from $Mo_{27}S_{50}$ to $Mo_{27}S_{48}$. In **11**, thiophene uprightly bonds with $Mo_{27}S_{50}$ through Mo_2 and Mo_3, in which the bond lengths of Mo_2S_T and Mo_3S_T are 2.542 and 2.539 Å, respectively. Furthermore, the distances of C_2–C_3 (1.439 Å) and C_1/C_4–S_T (1.764 Å/1.765 Å) are slightly elongated and that of C_1–C_2 (1.318 Å) is slightly shortened relative to those of free thiophene (1.730, 1.347 and 1.424 Å for C_1–S_T, C_1–C_2 and C_2–C_3). The low adsorption energy of thiophene (−5.1 kcal/mol) in Table 1 also indicates that the adsorption of thiophene at 3-fold CUS is weak. In contrast, **12** is obtained when thiophene is flatly placed above Mo_2 and Mo_3 of **8**. As shown in **12**, thiophene is pushed away from ($\bar{1}$ 0 1 0) edge with long distances of Mo_2–S_T and Mo_3–S_T (4.528 and 4.276 Å, respectively). The bond lengths of adsorbed thiophene changes (slightly). The positive adsorption energy (16.8 kcal/mol) of thiophene further proves that the structure **2** is unstable.

At the sulfur vacancies of **9**, three optimized structures (**13**, **14** and **15**) are obtained (in Fig. 3). In **13** with uprightly adsorbed thiophene at Mo_1 and Mo_2, the distances of Mo_1S_T and Mo_2S_T are 2.530 and 2.527 Å, respectively. All bond lengths of C_1–S_T, C_1–C_2 and C_2–C_3 of thiophene are elongated compared with free thiophene. In **14**, thiophene flatly adsorbs between Mo_1–Mo_2 to form 3-fold coordinated structure (η^1, S_T, η^2 and C). The bond lengths of Mo_1–S_T, Mo_2–C_2 and Mo_3–C_3 are 2.470, 2.306 and 2.310 Å, respectively. The adsorbed thiophene is strongly deformed, in which the S_T atom is titled over the plane of thiophene. Relative to the bond length free thiophene, the bond lengths of C_1–S_T and C_1–C_2 are elongated to 1.853–1.855 and 1.444–1.446 Å, while that of C_2–C_3 changes slightly. At the site between Mo_2–Mo_3, only the flat adsorption of thiophene (**15**) with 5-fold (η^1, S_T, η^4, C) coordinated structure is possible, and the uprightly adsorption configuration is not stable. The bond lengths of S_T–Mo_3, C_1–Mo_2 and C_2–Mo_2 in **15** are 2.685, 2.285–2.289 and 2.339–2.340 Å, respectively. Similar to **14**, the adsorbed thiophene in **15** is also strongly deformed with S_T tipping from the thiophene ring and the bond length of C_1–S_T, C_1–C_2 are elongated to 1.824–1.826 and 1.427–1.430 Å and that of C_2–C_3 changes (slightly). As given in Table 1, the adsorption energy decreases as the sequence of **14**, **15** and **13**.

16 and **17** are optimized structures of thiophene adsorbed at the $Mo_{27}S_{48}$ cluster. In **16**, thiophene uprightly bonded with Mo_1 and Mo_2, and the bond lengths of Mo_1–S_T and Mo_2–S_T are 2.532 and 2.499 Å, respectively. Similar to thiophene adsorption at $Mo_{27}S_{49}$, (**13** and **14**), all bond lengths of C_1–S_T, C_1–C_2 and C_2–C_3 of **16** are weakly elongated by 0.028–0.039, 0.011–0.149 and 0.019 Å, respectively. While in **17**, thiophene is flatly adsorbed over the 4-fold Mo_1 and Mo_2 CUS. The distance of Mo_1–C_1 is 2.402 Å and those of Mo_1–C_2 and Mo_1–C_3 are 2.273–2.275 Å. Furthermore, the bond lengths of C_1–S_T, C_1–C_2 of **17** are greatly elongated by 0.139–0.149 Å and that of C_2–C_3 only changes slightly.

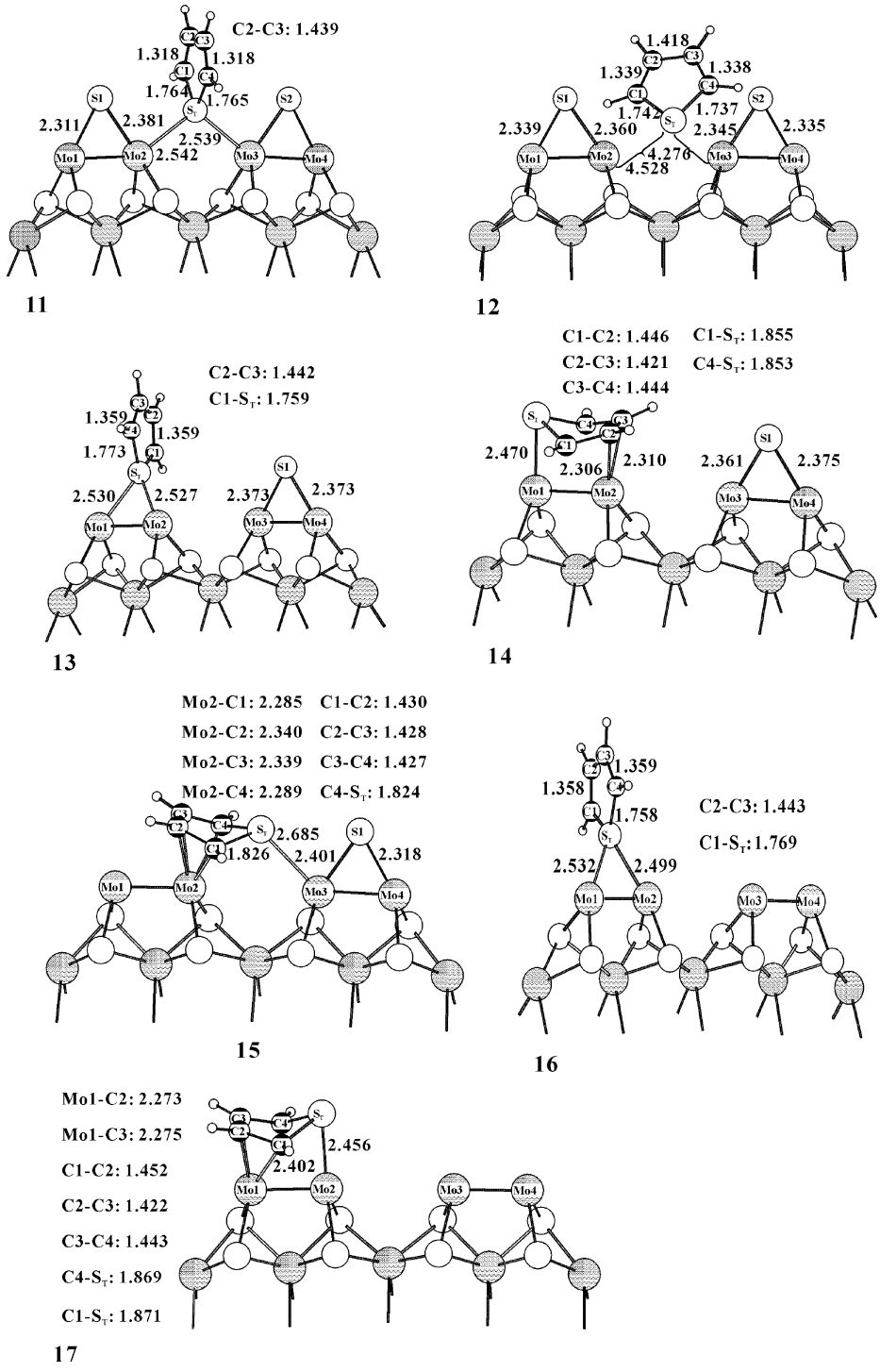

Fig. 3. Optimized structures of thiophene adsorbed on the vacancies of MoS_2.

4. Discussion

Experimental results have revealed that the properly reduced edges (especially for 3- or 4-fold coordination unsaturation sites) are responsible for the HDS activities [1–4,9]. From Fig. 1, it is found there are two types of edge (i.e. (1 0 $\bar{1}$ 0) and ($\bar{1}$ 0 1 0)) on the $Mo_{27}S_{54}$ cluster [5,27]. Surface science experimental results and theoretical calculations have shown that the formation of CUS with the removal of S starts with the terminal S atoms on the (1 0 $\bar{1}$ 0) and ($\bar{1}$ 0 1 0) edges [28–30]. The terminal S atoms on the (1 0 $\bar{1}$ 0) surface can be removed even by molecular hydrogen, however 3- or 4-fold CUSs are difficult to form on (1 0 $\bar{1}$ 0) edge because this process needs the removal of S atoms bound to three Mo atoms and completely destroys the MoS_2 structure. This deep reduction of MoS_2 is prevented in HDS process by introducing small amount of H_2S [3–5]. In contrast, 3- or 4-fold CUSs are easily formed on the ($\bar{1}$ 0 1 0) edge by only removing the bridging S atoms at the HDS reaction conditions. Kasztelan

Table 2
The enthalpy (kcal/mol) for formation of vacancies ($Mo_{27}S_{54-x}$ (x = 1–6)) under the treatment of molecular and atomic hydrogen

Reaction		Energy change
$Mo_{27}S_{54}$(**1**) + H_2 → $Mo_{27}S_{53}(S_5, \mathbf{2})$ + H_2S	(1)	4.0
$Mo_{27}S_{54}$(**1**) + 2H → $Mo_{27}S_{53}(S_5, \mathbf{2})$ + H_2S	(2)	−100.9
$Mo_{27}S_{54}$(**1**) + H_2 → $Mo_{27}S_{53}(S_3, \mathbf{3})$ + H_2S	(3)	14.7
$Mo_{27}S_{54}$(**1**) + 2H → $Mo_{27}S_{53}(S_3, \mathbf{3})$ + H_2S	(4)	−90.2
$Mo_{27}S_{53}(S_5, \mathbf{2})$ + H_2 → $M_{27}S_{52}(S_{1,5}, \mathbf{4})$ + H_2S	(5)	−27.6
$Mo_{27}S_{53}(S_5, \mathbf{2})$ + 2H → $M_{27}S_{52}(S_{1,5}, \mathbf{4})$ + H_2S	(6)	−132.4
$Mo_{27}S_{53}(S_5, \mathbf{2})$ + H_2 → $M_{27}S_{52}(S_{5,6}, \mathbf{5})$ + H_2S	(7)	41.5
$Mo_{27}S_{53}(S_5, \mathbf{2})$ + 2H → $M_{27}S_{52}(S_{5,6}, \mathbf{5})$ + H_2S	(8)	−63.3
$M_{27}S_{52}(S_{1,5}, \mathbf{4})$ + H_2 → $Mo_{27}S_{51}(S_{1,3,5}, \mathbf{6})$ + H_2S	(9)	6.7
$M_{27}S_{52}(S_{1,5}, \mathbf{4})$ + 2H → $Mo_{27}S_{51}(S_{1,3,5}, \mathbf{6})$ + H_2S	(10)	−98.1
$Mo_{27}S_{51}(S_{1,3,5}, \mathbf{6})$ + H_2 → $Mo_{27}S_{50}(S_{1-3,5}, \mathbf{7})$ + H_2S	(11)	42.2
$Mo_{27}S_{51}(S_{1,3,5}, \mathbf{6})$ + 2H → $Mo_{27}S_{50}(S_{1-3,5}, \mathbf{7})$ + H_2S	(12)	−62.6
$Mo_{27}S_{51}(S_{1,3,5}, \mathbf{6})$ + H_2 → $Mo_{27}S_{50}(S_{1,3-5}, \mathbf{8})$ + H_2S	(13)	30.8
$Mo_{27}S_{51}(S_{1,3,5}, \mathbf{6})$ + 2H → $Mo_{27}S_{50}(S_{1,3-5}, \mathbf{8})$ + H_2S	(14)	−74.0
$Mo_{27}S_{50}(S_{1,3-5}, \mathbf{8})$ + H_2 → $Mo_{27}S_{49}(S_{1-5}, \mathbf{9})$ + H_2S	(15)	52.6
$Mo_{27}S_{50}(S_{1,3-5}, \mathbf{8})$ + 2H → $Mo_{27}S_{49}(S_{1-5}, \mathbf{9})$ + H_2S	(16)	−52.2
$Mo_{27}S_{49}(S_{1-5}, \mathbf{9})$ + H_2 → $Mo_{27}S_{48}(S_{1-6}, \mathbf{10})$ + H_2S	(17)	54.7
$Mo_{27}S_{49}(S_{1-5}, \mathbf{9})$ + 2H → $Mo_{27}S_{48}(S_{1-6}, \mathbf{10})$ + H_2S	(18)	−50.2

et al. [31,32] find the correlation between catalytic activity and the extent of reduction of MoS_2 catalysts, which further confirms that the CUSs on the reduced ($\bar{1}$ 0 1 0) edges of MoS_2 slabs are responsible for the activity of HDS. More specifically, 3-fold CUSs involving SH groups would be the main active sites for HDS catalysis [5,7].

It is interesting and necessary to compare the enthalpy for the formation of vacancies for clusters deduced from **1** during the treatment under hydrogen atmosphere (see Table 2), since catalyst reduction is one of the most important steps in the catalyst life cycle [1–4]. The enthalpies of formation of vacancies due to the reaction of the $Mo_{27}S_{(54-x)}$ clusters and H_2/H to form products (reduced $Mo_{27}S_{(54-x-1)}$ and H_2S) are listed in Table 2. It is found that reactions (1) and (9) are slightly positive (4.0–6.7 kcal/mol) and reaction (5) is negative (−27.6 kcal/mol), indicating that the formation of the corresponding reduced structures is thermodynamically possible for the molecular hydrogen agent at the real HYD/HDS condition, for example, the high pressure of hydrogen and elevated temperature. Compared to the other cases, reactions (3) and (7) show high positive enthalpy (14.7 and 41.5 kcal/mol), indicating that this type of sulfur vacancy is relatively difficult to form. The negative enthapies of reactions (2), (4), (6), (8) and (10) show that formations of corresponding reduced structure are thermodynamically favorable for atomic hydrogen.

The enthalpy further increases in the sequence of reactions (13) < (15) < (17), implying that the formation of 3- and 4-fold CUS is more difficult with molecular hydrogen for reduction. This result is also in line with the conclusions by Raybaud et al. [10–13], who found that the S coverage of S-terminated edge could vary between 100% and 50% under different H_2/H_2S atmosphere. However, the role of atomic hydrogen is not taken into account in the Raybaud's thermodynamic model. Although the enthalpy also increases in the sequence of reactions (14) < (16) < (18), these energy changes remain negative for atomic hydrogen. Therefore, atomic hydrogen can nearly always accelerate the formation of all types of vacancies, which is in agreement with the experimental results [5]. In laboratory work and in industrial practice, the promoters such as Co and Ni are often added to improve the performance of MoS_2 catalysts. The remote control theory [33,34] proposes that cobalt sulfide promoters supply a sufficient amount of atomic hydrogen species to create more 3-fold and perhaps the majority of 4-fold CUS sites on the MoS_2 edge.

It is informative to compare the changes between the highest occupied (HOMO) and the lowest unoccupied (LUMO) molecular orbitals, which are analyzed by DFT calculations. As shown in Fig. 4, the occupied frontier orbitals are located at the vacancy sites on both Mo and S in **2**, **4**, **6** and **7** with lower coordination unsaturated sites, while the higher coordination unsaturated sites in **8**, **9** and **10** do not contribute the occupied frontier orbitals. This indicates that lower coordination unsaturated sites can donate electrons as Lewis base for catalytic reactions.

In addition, we also analyzed the LUMO and LUMO + 1. As shown in Fig. 5, the highly coordination unsaturated sites in **8**, **9** and **10** contribute significantly to the unoccupied frontier orbital, while there are no contributions from the lower coordination unsaturated site. This indicates that higher coordination unsaturated sites can accept electrons as Lewis acid for catalytic reactions. Therefore, the catalytic properties of molybdenum sulfide depend on the preparations, especially on the reduction period. For HDS reaction, the cleavage of S–C bonds demands the interaction of the HOMO portion of the S atom in thiophene with the LUMO of the metal site [35,36]. On the basis of the previous results, **8**, **9** and **10** might be more important active sites in HSD reaction.

Because adsorption of thiophene on the S-terminated edge is always endothermic [10], the CUS must be formed in order to adsorb and activate thiophene molecule on the ($\bar{1}$ 0 1 0) plane. It is also found that even at 3-fold CUS of **8**, the flatly adsorbed

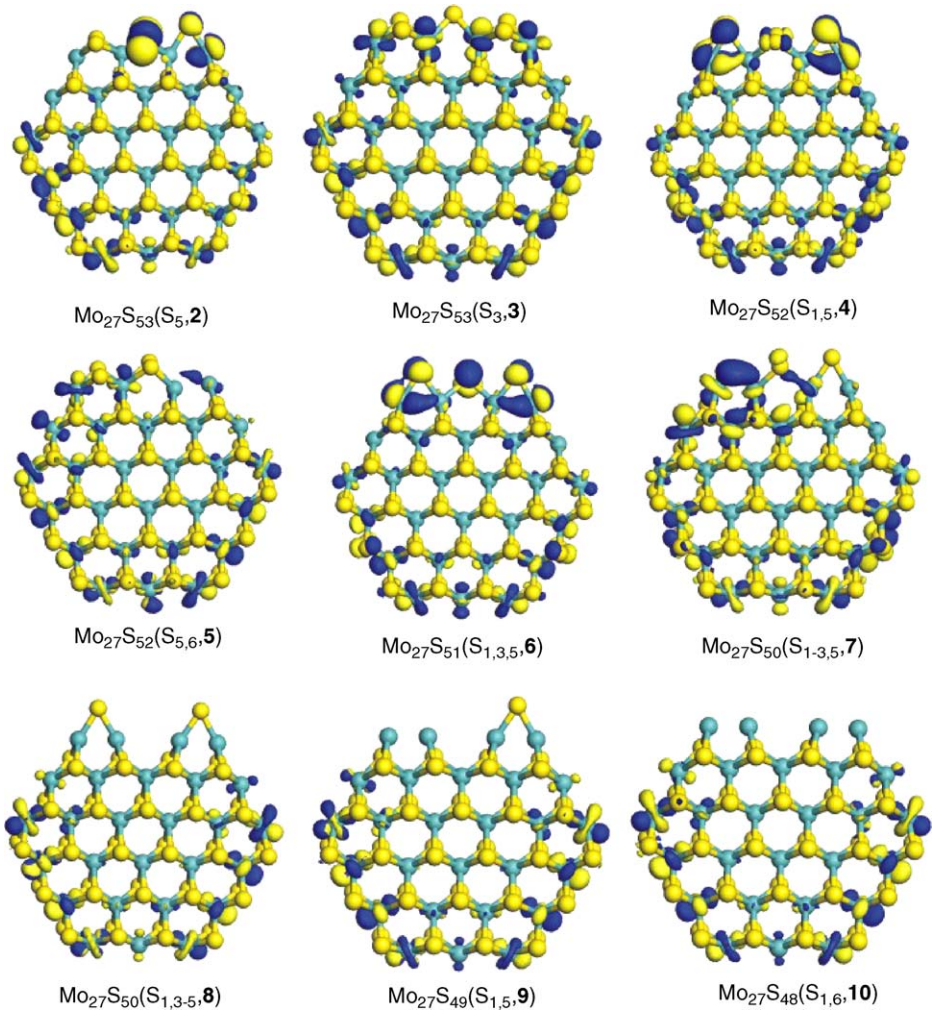

Fig. 4. Isosurface of the combined HOMO and HOMO-1 of $Mo_{27}S_{54-x}$ cluster.

configuration of thiophene (**12**) is not stable with the positive adsorption energy and the structure of thiophenen slightly changes due to the long optimized distance between thiophene and adsorbed sites. The upright adsorption configuration is relatively stable, the change trend of adsorbed thiophene is the same as the results of IR [37] and other theoretical results [20], but the disturbance of thiophene in **11** is still very weak. Therefore, it is necessary to remove more sulfur atoms to form 4-fold CUS for activation of thiophene.

On the basis of the configure of thiophene uprightly adsorbed between the two vicinal 4-fold CUS (Mo_1 and Mo_2) (**13** and **16**), it is found that all bond length of S_T–C_α, C_α–C_β and C_β–C_β are elongated by 0.028–0.043, 0.011–0.012 and 0.018–0.019 Å, respectively. It is noticeable that the bond length of C_α–C_β also increases, disagreement with the results of uprightly adsorbed thiophene at other sites [20,37]. The mild change of bond length of upright adsorbed thiophen further indicates that the activation of thiophene is activated at a low degree. In contrast, the thiophene is strongly activated and the aromaticity is destroyed when thiophene are adsorbed flatly between two vicinal 4-fold CUS (**14**, **17**) or between 3- and 4-fold CUS (**15**). The S_T atom is bent from thiophene ring and the bond length of S_T–C_α, C_α–C_β are elongated by 0.094–0.141 and 0.080–0.105 Å, respectively. This value is more evident than that in thiophene adsorbed at the 2-fold CUS of $(1\,0\,\bar{1}\,0)$ of MoS_2 [20]. However, the rupture of S_T–C_α is not observed in all models employed here.

It is useful and informative to analyze the atomic charge which always includes the information of structure change and thiophene activation. The Hirshfeld charge [38] is defined relative to the deformation density which is the difference between the molecular and the unrelaxed atomic charge densities. Comparing with the change of Hirshfeld charge (see Table 3), it is found that the charge transfers from thiophene to substrate for the uprightly adsorbed configuration (**11**, **13** and **16**). The net charge transfer is 0.272, 0.143 and 0.135 for **11**, **13** and **16**, respectively. However, the adsorption energy of thiophene increases as the sequence of **11**, **13** and **16**, which implies that the back-donation of Mo atoms to thiophene might cause the adsorbed configuration more stable. This suspicion can be further evidenced by the change of local atomic charge. In structure **11**, Mo_2 or Mo_3 and Mo_1 or Mo_4 get 0.077–0.078 and 0.024–0.026 electron, respectively, illustrating Mo_2 and Mo_3 atoms transfer the excess negative charge to the vicinal atoms (Mo_1 and Mo_4). In contrast, the negative charge mainly locates on the Mo_1 and

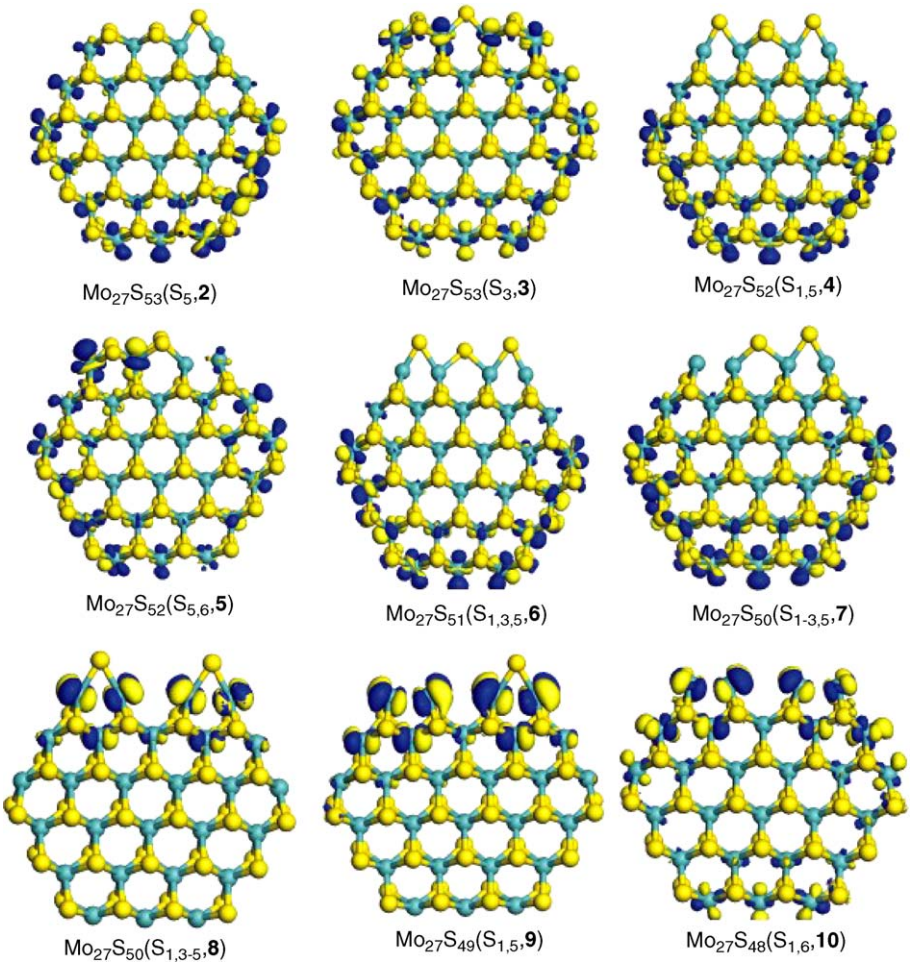

Fig. 5. Isosurface of the combined LUMO and LUMO + 1 of $Mo_{27}S_{54-x}$ cluster.

Mo_2 atoms and the positive charge of S_T of thiophene is much lower in cluster **13**, **16**, suggesting the evident back-donation effect from Mo to S_T. It is well known that the electron donation and back-donation of thiophene accomplish through the lone pair of S_T of thiophene in uprightly adsorbed thiophene. From the composition of the frontier orbitals of thiophen (Fig. 6), it is found that the orbits of 1a1 and 2b1 can donate electron while that of 1b2 and 3b1 can accept electron through the S_T atom. Because the energy of 2b1 and 1a1 are remarkably lower than that of HOMO (−5.947 eV), the donation of thiophene through this mode is weak and then the back-donation of thiophene is also low, which causes thiophene activated at low degree.

In flat adsorbed structure, the 0.037 and 0.058 net charge transfer from thiophene to substrate in **14**, **15**, which is much

Table 3
The Hirshfeld charge population of optimized cluster

	11	**12**	**13**	**14**	**15**	**16**	**17**
Mo_1	−0.026	−0.014	−0.044	−0.018	0.026	−0.034	−0.008
Mo_2	−0.078	0.007	−0.015	0.007	−0.007	−0.022	0.032
Mo_3	−0.077	0.004	0.024	0.02	−0.042	0.000	0.003
Mo_4	−0.024	−0.013	−0.013	−0.012	−0.021	−0.013	−0.001
S_1	−0.001	0.012	−0.009	−0.006	0.011		
S_2	−0.001	0.010					
S_T	0.052	0.015	−0.002	0.022	0.025	−0.004	−0.005
C_1	0.032	0.008	0.012	−0.004	−0.021	0.019	−0.007
C_2	0.040	0.001	0.031	−0.011	0.011	0.03	−0.011
C_3	0.039	0.001	0.033	−0.01	0.012	0.027	−0.015
C_4	0.032	−0.004	0.02	−0.003	−0.019	0.009	−0.012
Substrate	−0.272	−0.011	−0.143	−0.037	−0.058	−0.135	0.004
Adsorbate	0.273	0.013	0.144	0.038	0.057	0.136	−0.004

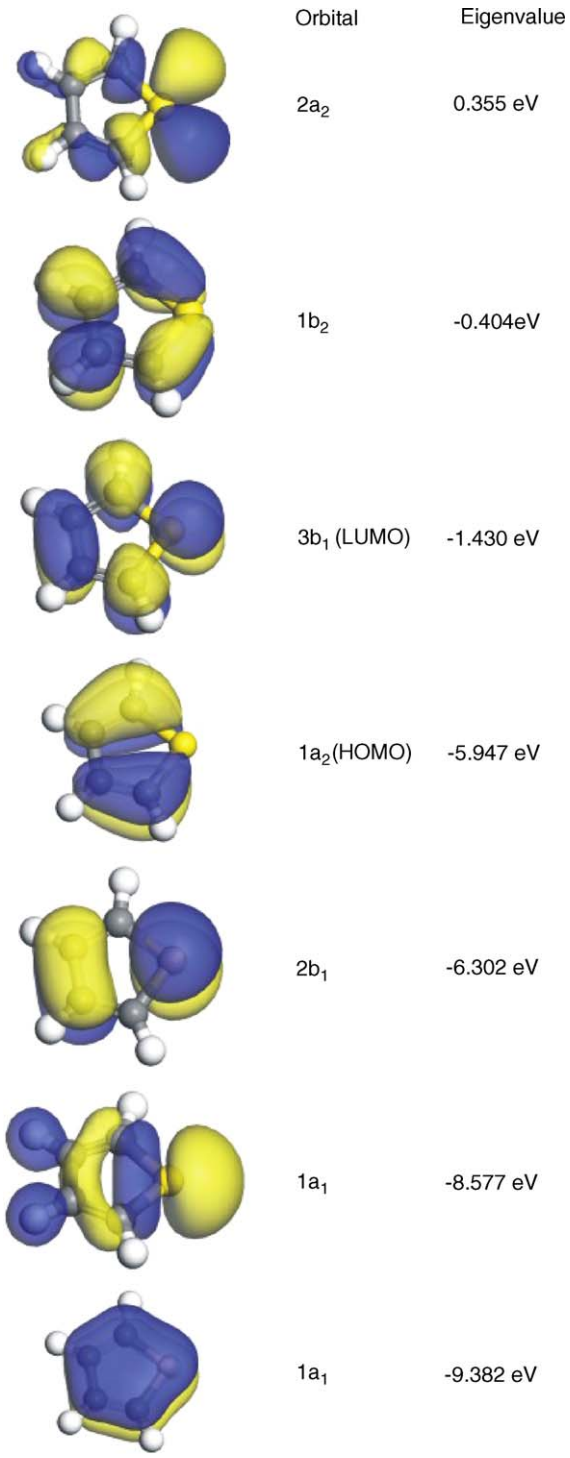

Fig. 6. Isosurface of different orbitals of thiophene.

lower than that in **11**, **13**, **14**, while 0.004 net charge in **7** transfers in the reverse direction. This cannot illustrate the weak interaction between thiophene and substrate because of much larger adsorption energy and strong disturbance of thiophene in these configures. Only the electron donation and back-donation can account for the activation of thiophene in flatly adsorbed structure because all C_α, C_β and S_T can participate in the electron donation and back-donation in these adsorbed configuratons. From the frontier orbitals of thiophene (shown in Fig. 6), it is feasible that the HOMO (1a2) of thiophene donates electron and LUMO (3b1) of thiophene accepts the electron, which can be responsible for the weakening bonds and the increased distances of C_α–C_β and S_T–C_α.

Because all the CUSs do not be sufficient for C–S bond cleavage, the hydrogen is necessary for the rapture of S_T–C_α. Delmon and Froment [1] and Startsev [3] believe that the hydrogen or proton concentration near the active sits is crucial for the catalytic activity of thiophene hydrogenation. Hadjiloizou et al. [9] also propose that the strongly acidic sites including SH is responsible for the activity for thiophene HDS. We also put a hydrogen molecule between S_T and S1of **15**, and get the optimized structure in which the H_2 molecule is dissociatively adsorbed to form -S_TH and S_1H. When H of S_TH transfers to C4, the cleavage of C4–S_T is observed [39]. In the concerted mechanism of thiophene hydrogenolysis, it is considered that the excess negative charges transfer from thiophene to substrate are located on the coordinative unsaturated S atoms in the $(\bar{1}\,0\,1\,0)$ plane, compensation for this charge will be possible by dissociative adsorption of the dihydrogen molecule [3,4]. However, the data shown in Table 3 show that the atomic change of S1 or S2 in **11**, **13**, **4** and **15** is mild. Even so, the vacancy of $Mo_{27}S_{49}$ is important for thiophene hydrogenolysis not only because this site can effectively activate the thiophene, but also because the S1 atom of this cluster bearing −0.245 to 0.262 charge is active to dissociatively adsorb the hydrogen molecule. The hydrogenation of thiophen at this site will be carried out in the future work.

5. Conclusion

The various structures of bridging sulfur vacancies on the $(\bar{1}\,0\,1\,0)$ edge of $Mo_{27}S_{(54-x)}$ are optimized using density functional theory. The theoretical results represent that clusters **2**, **4** and **8** are more stable than **3**, **5** and **7**. The distances between Mo_1–Mo_2 or/and between Mo_3–Mo_4 become shortened to form bonds with the loss of corner sulfur atoms while the distance between Mo_2–Mo_3 increases with the removal of edge sulfur atoms.

On the basis of the frontier molecular orbitals, a possible site for activation of thiophene might be situated between vicinal 4-fold CUS.

From the enthalpy for vacancy formation, it is concluded that the vacancies of $Mo_{27}S_{(54-x)}$ ($x = 1$–3) are easily formed during the treatments with molecular (under the normal HYD/HDS condition) or atomic hydrogen. However, the formation of $Mo_{27}S_{(54-x)}$ ($x = 4$–6) clusters is always difficult using molecular hydrogen while it can be accelerated by atomic hydrogen

The adsorption of thiophene at the various vacancies on the $(\bar{1}\,0\,1\,0)$ edge of MoS_2 is optimized using density functional theory. On the basis of the theoretical results, it is found **12** is unstable compared with other clusters. The uprightly adsorbed thiophene in **11**, **13** and **16** is activated at the limited degree while the flatly adsorbed one in **4**, **5** and **7** is strongly activated.

According to Hirshfeld charge analysis, the donation and back-donation between the thiophene and the substrate might be responsible for the activation of thiophene.

Acknowledgements

The financial supports from National Science Foundation of China (Grant No. 20503005) and from the Natural Science Foundation of Shanxi Province, China (Grant No. 20031022) are gratefully acknowledged.

References

[1] B. Delmon, G.F. Froment, Catal. Rev. Sci. Eng. 38 (1996) 69.
[2] H. Topsøe, B.S. Clausen, F.E. Franklin, E. Massoth, in: J.R. Anderson, M. Boudart (Eds.), Science and Technology in Catalysis: Hydrotreating Catalysis, vol. 11, Springer, Berlin, 1996.
[3] A.N. Startsev, Catal. Rev. Sci. Eng. 37 (1995) 353.
[4] A.N. Startsev, J. Mol. Catal. 152 (2000) 1.
[5] S.Y. Li, J.A. Rodriguez, J. Hrbek, H.H. Huang, G.-Q. Xu, Surf. Sci. 366 (1996) 29.
[6] Y.I. Yermakov, A.N. Startsev, V.A. Burmistrov, O.N. Shumilo, N.N. Bulgakov, Appl. Catal. 18 (1985) 33.
[7] Y.-W. Li, X.-Y. Pang, B. Delmon, J. Mol. Catal. A 169 (2001) 259.
[8] Y.-W. Li, X.-Y. Pang, B. Delmon, J. Phys. Chem. A 104 (2000) 11375.
[9] G.C. Hadjiloizou, J.B. Butt, J.S. Dranoff, Ind. Eng. Chem. Res. 31 (1992) 2503.
[10] P. Raybaud, J. Hafner, G. Kresse, H. Toulhoat, Phys. Rev. Lett. 80 (1998) 1481.
[11] P. Raybaud, J. Hafner, G. Kresse, H. Toulhoat, Surf. Sci. 407 (1998) 237.
[12] P. Raybaud, J. Hafner, G. Kresse, S. Kasztelan, H. Toulhoat, J. Catal. 190 (2000) 128.
[13] P. Raybaud, J. Hafner, G. Kresse, S. Kasztelan, H. Toulhoat, J. Catal. 189 (2000) 129.
[14] H. Schweiger, P. Raybaud, G. Kresse, H. Toulhoat, J. Catal. 207 (2002) 76.
[15] M.V. Bollinger, K.W. Jacobsen, J.K. Nϕrskov, Phys. Rev. B 67 (2003) 085410.
[16] J.-F. Paul, E. Payen, J. Phys. Chem. B 107 (2003) 4057.
[17] H. Orita, K. Uchida, N. Itoh, J. Mol. Catal. A 195 (2003) 173.
[18] P. Faye, E. Payen, D. Bougeard, J. Mol. Model. 5 (1999) 63.
[19] X. Ma, H.H. Schobert, J. Mol. Catal. A 160 (2000) 409.
[20] H. Orita, K. Uchida, N. Itoh, J. Mol. Catal. A 193 (2003) 197.
[21] H. Yang, C. Fairbridge, Z. Ring, Energy Fuels 17 (2003) 387.
[22] Y. Inoue, Y. Uragami, Y. Takahashi, S. Eijsbouts, Science and Technology in Catalysis 1998, Kodansha Ltd., Tokyo, 1999, pp. 415–418.
[23] B. Delley, J. Chem. Phys. 92 (1990) 508.
[24] B. Delley, J. Phys. Chem. 100 (1996) 6107.
[25] B. Delley, J. Chem. Phys. 113 (2000) 7756.
[26] R.W.G. Wyckoff, Crystal Structure, vol. 1, second ed., John Wiley & Sons, New York, 1964, pp. 280–281.
[27] Y.I. Yermakov, A.N. Startsev, V.A. Burmistrov, O.N. Shumilo, N.N. Bulgakov, Appl. Catal. 18 (1985) 33.
[28] W. Qian, A. Ishihara, G. Wang, T. Tsuzuki, M. Godo, T. Kabe, J. Catal. 170 (1997) 286.
[29] W. Qian, A. Ishihara, Y. Aoyama, T. Kabe, Appl. Catal. A 196 (2000) 103.
[30] D. Wang, W. Qian, A. Ishihara, T. Kabe, J. Catal. 209 (2002) 266.
[31] S. Kasztelan, J. Jalowiecki, A. Wambeke, J. Grimblot, J.P. Bonnelle, Bull. Soc. Chim. Belg. 96 (1987) 1003.
[32] S. Kasztelan, H. Toulhoat, J. Grimblot, J.P. Bonnelle, Appl. Catal. 13 (1984) 127.
[33] B. Delmon, Int. Chem. Eng. 20 (1980) 369.
[34] B. Delmon, Surf. Rev. Lett. 2 (1995) 25.
[35] X. Ma, H.H. Schobert, Prepr., Div. Petrol. Chem., ACS 42 (1997) 657.
[36] C.L. Marshall, J.R. Brenner, J.L. Tilson, M.L. Palmer, Div. Petrol. Chem., ACS, Dallas, TX, March 29–April 3, 1998, pp. 28–31.
[37] T.L. Tarbuck, K.R. McCrea, J.W. Logan, J.L. Heiser, M.E. Bussell, J. Phys. Chem. B 102 (1998) 7845.
[38] F.L. Hirshfeld, Theor. Chim. Acta B 44 (1977) 129.
[39] Unpublished results.